Variance-Reduction Techniques for Disconnected Isospin-Breaking QED Corrections

Ryan Hill

RBC-UKQCD

7$^{\mathrm{th}}$ June 2024
Riken Center for Computational Science Seminar

THE UNIVERSITY *of* EDINBURGH

Talk Outline

- Motivation
- Lattice Strategy for $P \to \ell\overline{\nu}$
- Applications to rare $K^+ \to \pi^+\ell^+\ell^-$ decays
- Conclusions

Motivation

- FLAG[1] reports averages for observables calculable from $K \to \ell\overline{\nu}$, $\pi \to \ell\overline{\nu}$ at a sub-percent level.
  - $N_f = 2+1$ $\quad f_{\pi^\pm} = 130.2(0.8)$ MeV (0.61%)
  - $N_f = 2+1+1$ $\quad f_{K^\pm} = 155.7(0.3)$ MeV (0.19%)
  - $N_f = 2+1$ $\quad f_{K^\pm} = 155.7(0.7)$ MeV (0.45%)
- These inform $|V_{us}|/|V_{ud}|$.
- PDG 2024[2] reports a 2.3σ tension in $|V_{ud}|^2 + |V_{us}|^2 + |V_{ub}|^2$.

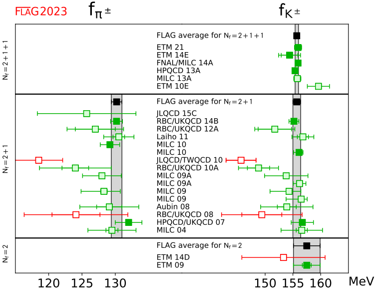

- Lattice results based on partial evaluation of first-order isospin-breaking corrections (or χPT).
- $< 1\%$ errors without a full *ab-initio* correction?

Plot from FLAG Review 2021 (February 2024 Revision). Full citation list at end of talk.

[1] FLAG Review 2021 (February 2024 Revision), http://flag.unibe.ch/2021/

[2] Navas *et al.* (Particle Data Group), to be published in PRD 110 (2024) 030001

Motivation

- Similar situation for $D \to \ell\overline{\nu}$, $D_s \to \ell\overline{\nu}$.
  - $N_f = 2+1+1$ $f_D = 212.0(0.7)$ MeV (0.33%)
  - $N_f = 2+1$ $f_D = 209.0(2.4)$ MeV (1.15%)
  - $N_f = 2+1+1$ $f_{D_s} = 249.9(0.5)$ MeV (0.2%)
  - $N_f = 2+1$ $f_{D_s} = 248.0(1.6)$ MeV (0.65%)

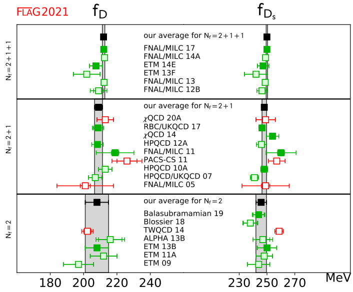

- Important to include a complete *ab-initio* calculation of first-order isospin-breaking corrections.

Plot from FLAG Review 2021 (February 2024 Revision). Full citation list at end of talk.

Motivation: Isospin-Breaking Corrections to $P \to \ell\overline{\nu}$

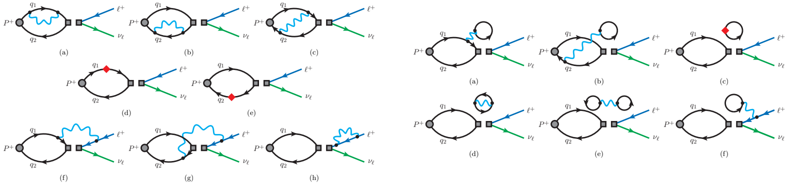

Diagrams from Boyle *et al.* JHEP 02 (2023) 242. Red diamonds: scalar insertions.

- Quark-connected contributions (left) to the isospin-breaking correction have been calculated for $P \to \ell\overline{\nu}$ in lattice QCD[1] [2].
- Quark-disconnected contributions (right) omitted.
- Referred to as the "electro-quenched" approximation.
- Uncontrolled systematic.

[1] Di Carlo *et al.* PRD 100 (2019) 034514 [arXiv:1904.08731]

[2] Boyle *et al.* JHEP 02 (2023) 242 [arXiv:2211.12865]

Motivation: Size of Quark-Disconnected Diagrams

- BMW 2020 g_μ-2 HVP paper[a] includes calculations of hadronic $\mathcal{O}(\alpha)$ IB quark-connected **and** quark-disconnected sub-diagrams relevant to $P \to \ell\overline{\nu}$.
- Quark-disconnected is 30% of $\mathcal{O}(\alpha)$ IB quark-connected contribution here (small!).
- Contribution not known for $P \to \ell\overline{\nu}$.

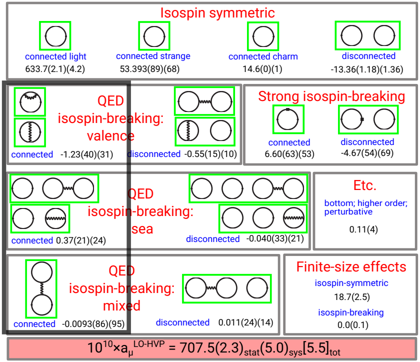

Diagram from Borsanyi *et al.* Nature 593, 51–55 (2021).
Grey box annotation not part of original image.

[a] Borsanyi *et al.* Nature 593, 51–55 (2021)

Motivation: Size of Quark-Disconnected Diagrams

- Large uncertainties on quark-disconnected diagrams.
- This is representative of the challenges involved in computing quark-disconnected diagrams.

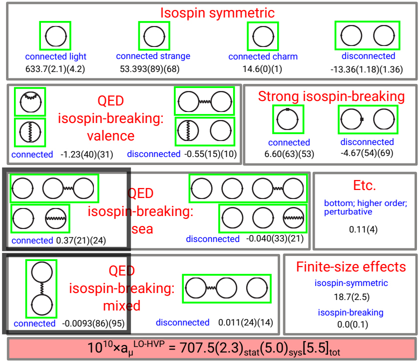

Diagram from [Borsanyi *et al.* Nature 593, 51–55 (2021)].
Grey box annotation not part of original image.

Motivation: Propagator Loops in Lattice QCD

- Quark-disconnected diagrams are difficult to estimate—loops given by factors like $D^{-1}(x,x)$.
- This requires one propagator solve per lattice site. $\rightarrow$ Computationally infeasible.
- Instead stochastically estimate Dirac operator inverse using noise vectors η obeying

$$\left\langle \eta(y)\eta^\dagger(x) \right\rangle_\eta = \delta_{xy}, |\eta(x)|^2 = 1, \langle \eta(x) \rangle_\eta = 0, \tag{1}$$

where $\langle \cdot \rangle_\eta$ is an average over η. This gives

$$D^{-1}(x,x) = \sum_y D^{-1}(x,y)\delta_{xy} \tag{2}$$

$$\approx \frac{1}{N_\eta} \sum_\eta \left(\sum_y D^{-1}(x,y)\eta(y) \right) \eta^\dagger(x). \tag{3}$$

Motivation: Propagator Loops in Lattice QCD

- The $\mathbb{Z}_2$ noise has been shown to be an optimal choice for estimating the trace of a Dirac matrix inverse[1].
- Elements randomly drawn from $\{1, -1\}$.
- However, stochastic estimators can make large contributions to the variance of quark-disconnected diagrams.
- Additional methods to reduce the variance are required.

[1] Dong, Liu. PLB 328 (1994). [arXiV:hep-lat/9308015]

Lattice Strategy

Lattice Strategy

- Working at $\mathcal{O}(\alpha)$: $m_u = m_d$.
- Introduce IB effects using the RM123 method[1] [2]:
  - IB corrections *via* perturbative expansion in $\alpha = \frac{e^2}{4\pi}$, m.

$$\langle O \rangle = \langle O \rangle \Big|_{e=0} + \underbrace{\frac{1}{2}\left(e^{\phi}\right)^2 \left[\frac{\partial}{\partial e}\frac{\partial}{\partial e}\langle O \rangle\right]_{e=0}}_{\text{QED IB}} + \underbrace{\left(m^{\phi} - m^{(0)}\right)\left[\frac{\partial}{\partial m}\langle O \rangle\right]_{e=0}}_{\text{Mass correction}} + \ldots \quad (4)$$

  - IB corrections take the form of additional diagrams evaluated in the isospin-symmetric limit.
  - m^{ϕ} = physical mass, m^0 = isospin-symmetric mass.
- $\mathcal{O}(\alpha) \sim \mathcal{O}(1\%) \Rightarrow$ IB required for sub-percent calculations.

[1] de Divitiis *et al.* JHEP 04 (2012) 124 [arXiv:1110.6294]

[2] de Divitiis *et al.* PRD 87 (2013) 114505 [arXiv:1303.4896]

Lattice Strategy: Ensemble Parameters

Pilot runs being performed on the RBC-UKQCD ‘C0’ ensemble.

- $2+1$ flavour, $L^3 \times T = 48^3 \times 96$, $a^{-1} = 1.73$ GeV.
- Physical-scale light-, strange-quark masses.
- zMöbius Domain-Wall action.
  $\rightarrow$ Cheaper than Möbius DWF; requires bias correction step.
  $\rightarrow$ Accumulate statistics on cheaper zMöbius estimator.
- Light quarks deflated with 2000 low modes.

Future runs to include ‘M0’ ensemble.

- 2+1 flavour, $L^3 \times T = 64^3 \times 128$, $a^{-1} = 2.36$ GeV.
- Also at physical-scale light-, strange-quark masses.

Calculation performed with **Grid**[1], and the Grid-based workflow management software **Hadrons**[2].

[1] https://github.com/paboyle/Grid
[2] https://github.com/aportelli/Hadrons

Lattice Strategy: Photon Action

- Finite volume + periodic boundary conditions:
  $\rightarrow$ Charged states forbidden by Gauss' Law.
- Need to choose a QED prescription.
  - QED$_L$: Remove spatial zero-mode[1].
    $\rightarrow$ Modern understanding: special case of QED$_L^{\mathrm{IR}}$ [2]
    $\rightarrow$ Large finite-volume effects at $\mathcal{O}(1/L^3)$ for $K \rightarrow \ell\overline{\nu}$?[3]
  - QED$_r$: Redistribute zero-mode to neighbouring modes[4] [5].
    $\rightarrow$ Designed to remove $\mathcal{O}(1/L^3)$ finite-volume effects from $K \rightarrow \ell\overline{\nu}$ and others
    $\rightarrow$ Also a particular case of QED$_L^{\mathrm{IR}}$

[1] Hayakawa and Uno, PTP 120 (2008) 413 [arXiv:0804.2044]
[2] Davoudi *et al.* PRD 99 (2019) 034510 [arXiv:1810.05923]
[3] Boyle *et al.* JHEP02(2023)242 arXiv: [2211.12865]
[4] Di Carlo, PoS LATTICE2023 (2024) 120 [arXiv:2401.07666]
[5] Hermansson-Treudsson *et al.*, PoS LATTICE2023 (2024) 265 [arXiv:2310.13358]

$\mathcal{O}(\alpha)$ Disconnected Diagrams for $P \to \ell\overline{\nu}$

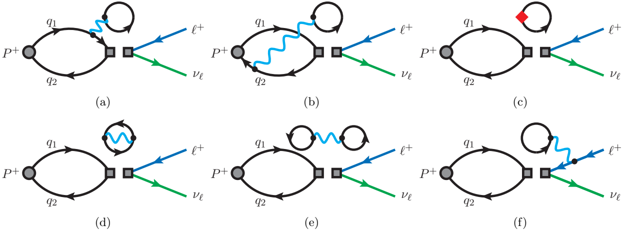

Diagrams from [Boyle *et al.* JHEP02(2023)242]. Red diamond: scalar insertions.

- Diagram (e): ‘Specs’ diagram.
- Diagrams (a), (b), (f): Tadpole diagrams.
- Diagram (d): ‘Burger’ diagram.
- Diagram (c): Sea-loop diagram (mass correction, real emission).

EM Current Insertions in the Isospin Limit

- $P \to \ell\overline{\nu}\ \mathcal{O}(\alpha)$ correlation function:

$$\sum_x \sum_y \langle J_\mu(x) A_\mu(x) J_\nu(y) A_\nu(y) O \rangle \tag{5}$$

- EM current insertions: $J_\mu(x) = \sum_f Q_f \overline{\psi}_f(x)\gamma_\mu\psi_f(x)A_\mu$.
  - $2+1f$: Consider sum over quark flavours $f \in \{u, d, s\}$.
  - Q_f: EM charge (*i.e.* $Q_u = 2/3$, $Q_d = -1/3$, $Q_s = -1/3$).
- Isospin limit: Partial cancellation between u and d.
- Light quark to represent u, d with charge $Q_{ud} = 1/3$.
- Light and strange quarks <u>equally-weighted</u>; relative minus sign.
- $\Rightarrow J_\mu(x) = 1/3\left(\overline{\psi}_l(x)\gamma_\mu\psi_l(x) - \overline{\psi}_s(x)\gamma_\mu\psi_s(x)\right)A_\mu$.

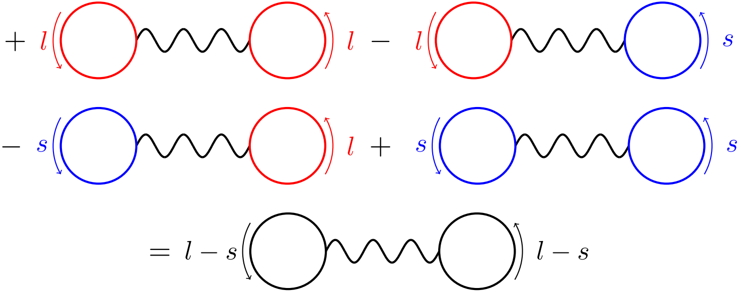

- Two independent loop flavours.
- l, s: generates four sub-diagrams with large cancellations.
- These can be factorised into a single diagram of $l - s$ propagators.

'Specs' — Split-Even Estimator

Giusti *et al.*[1] have demonstrated a successful variance-reduction strategy for differences of single-propagator loops: "split-even" estimators.

For *e.g.* Wilson, DWF Dirac Operators differing only by mass,

$$D_1^{-1} - D_2^{-1} = D_1^{-1}\left(D_2 - D_1\right) D_2^{-1}, \tag{6}$$

$$= (m_2 - m_1) D_1^{-1} D_2^{-1}. \tag{7}$$

Choice in how to stochastically estimate propagator traces:

$$\text{"Standard"} \quad (m_2 - m_1)\mathrm{Tr}\left\{\gamma^\mu \left\{D_1^{-1} D_2^{-1} \eta\right\}(x)\eta^\dagger(x)\right\}, \tag{8}$$

$$\text{"Split-Even"} \quad (m_2 - m_1)\mathrm{Tr}\left\{\gamma^\mu \left\{D_1^{-1}\eta\right\}(x)\{\eta^\dagger D_2^{-1}\}(x)\right\}, \tag{9}$$

[1] Giusti *et al.* EPJC 79, 586 (2019) [arXiv:1903.10447]

Split-Even

Split-even estimators have recently been used for:

- Pion scalar form factor Ottnad, von Hippel PoS LATTICE2023 (2024) 313
- $\pi^0 \to \gamma^*\gamma^*$ transition form factor Koponen *et al.*, PoS LATTICE2023 (2024) 254
  Gérardin *et al.* arXiv:2305.04570
- $\eta,\eta' \to \gamma^*\gamma^*$ transition form factors Gérardin *et al.* arXiv:2305.04570
- $g_\mu - 2$ Hadronic light-by-light Gérardin *et al.* arXiv:2305.04570
  Chao *et al.* EPJC 81 (2021) 7, 651
- Nucleon EM radii Djukanovic *et al.*, PRL 132 (2024) 21
- Nucleon EM form factors Djukanovic *et al.*, PRD 109 (2024) 9
- Nucleon Sigma terms Agadjanov *et al.* PRL 131 (2023) 26
- Hadronic running of EM coupling, EW mixing angle
  Cé *et al.* JHEP 08 (2022) 220

‘Specs’ — Estimator Comparison

- Application of ‘split-even’ to the ‘specs’ diagram explored at unphysical masses by Harris *et al.*[1].
- This work: application to physical masses.
- Preliminary tests at unphysical mass reproduce large improvement in statistical error.

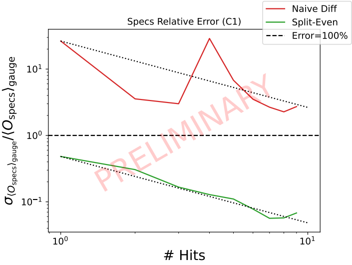

Plot from implementation tests.
Variance under gauge average on y axis.

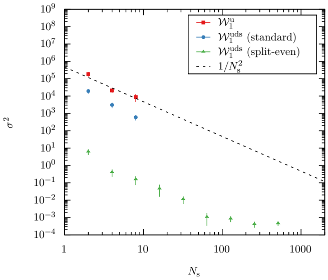

Plot from Harris *et al.*[1].
Variance under noise average on y axis.

[1] Harris *et al.* PoS LATTICE2022 (2023) 013 [arXiv:2301.03995]

‘Burger’ Diagram

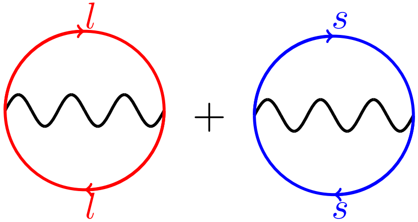

- Both propagators require the same flavour.
- No cancellation between l and s diagrams.
- Split-even can’t help here—a different approach is required.

'Burger' Diagram — Distance-splitting

$$\mathrm{Tr}\left\{D_q^{-1}(x,y)\gamma^\mu D_q^{-1}(y,x)\gamma^\nu\right\} G_{\mu\nu}(x-y) \tag{10}$$

- 'Burger' diagram falls off exponentially with propagator separation $\Rightarrow$ short-distance dominated.
- Harris *et al.*[1] take advantage of this by concentrating computational effort on short-distance behaviour.
  - Volume-averaged stochastic estimation of all-to-all propagators within a radius $|x-y| < R$.
  - Random point sources for $|x-y| >= R$.
- This work: currently working out some implementation details.

[1] Harris *et al.* PoS LATTICE2022 (2023) 013 [arXiv:2301.03995]

'Burger' Diagram — Distance-splitting

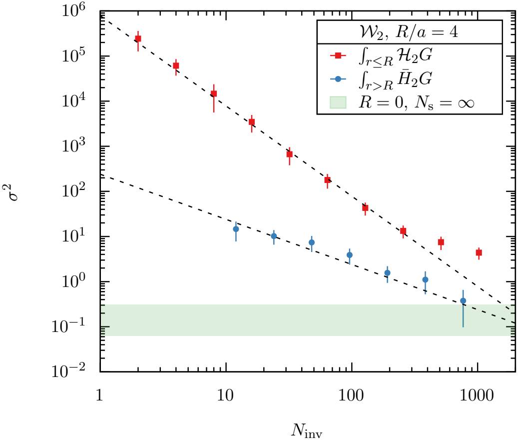

Plot from Harris *et al.*[1].

[1] Harris *et al.* PoS LATTICE2022 (2023) 013 [arXiv:2301.03995]

Tadpole Diagram

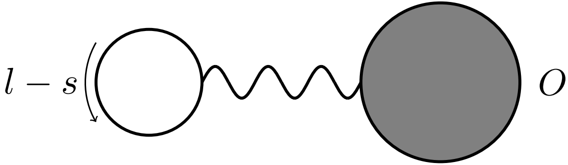

- Sea-quark loop photon-connected to propagator in subdiagram O.
- Similarly to the ‘specs’, the tadpole loop factorises to $l - s$.
- Tadpole can be calculated with a split-even estimator.
- Only $\mathcal{O}(\alpha)$ disc. diagram that contributes to mass splittings.
- This work: ongoing calculation effort.

Sea-loop Diagram

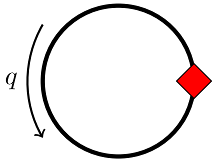

- Scalar insertion provides mass correction contribution.
- Vector insertion gives real photon emission.
  $\rightarrow$ This factorises into $q = (l - s)$ like the specs and tadpole.
  $\rightarrow$ Can also use split-even here.
- This work: ongoing calculation effort.

IB Corrections - Summary

- Quark-disconnected IB diagrams are challenging to compute.
- Omitting these diagrams is an uncontrolled systematic.
- Quark-disconnected IB diagrams with the split-even technique at physical masses new for $P \to \ell\overline{\nu}$.
- Harris *et al.*[1] find these techniques to be highly beneficial at non-physical mass.

[1] Harris *et al.* PoS LATTICE2022 (2023) 013 [arXiv:2301.03995]

Applications to rare $K^+ \to \pi^+ \ell^+ \ell^-$ decays

Another application: Rare Kaon Decays

- Rare $K^+ \to \pi^+\ell^+\ell^-$ decays feature diagrams with single-propagator loops—not dissimilar to disconnected QED diagrams.
- Decay amplitude A_0 hard to resolve at the physical point.
- Techniques used for disconnected QED have the potential to make a significant impact here.

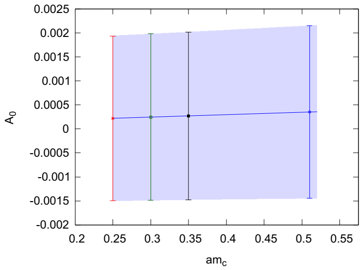

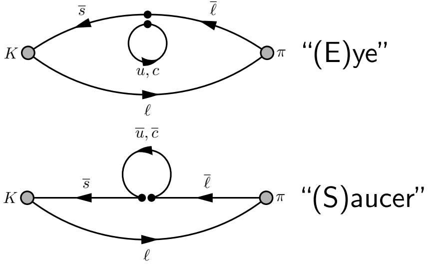

Plot from [Boyle *et al.* PRD 107 (2023) L011503]

$K^+ \to \pi^+ \ell\bar{\ell}$: Motivation

- $K \to \pi\ell\bar{\ell}$ decays proceed *via* flavour-changing neutral current.
  $\to$ Highly suppressed; sensitive to new physics.
- CP-conserving processes dominated by virtual-γ-exchange[1].
  $\to$ Primarily long-distance quantities.
  $\to$ Well-suited to lattice QCD techniques.
- $K_S \to \pi^0\ell^+\ell^-$ very experimentally challenging.
  $\to$ Focus lattice calculations on $K^+ \to \pi^+\ell^+\ell^-$.
- Previous RBC-UKQCD physical-point calculation dominated by GIM-loop uncertainties[2].
  $\to$ Efficient estimation of these should translate to a more precise A_0 calculation.

[1] D'Ambrosio *et al.* JHEP 08 (1998) 004 [arXiv:hep-ph/9808289]
[2] Boyle *et al.* PRD 107 (2023) L011503 [arXiv:2202.08795]

$K^+ \to \pi^+\ell^+\ell^-$: Preliminary split-even variances

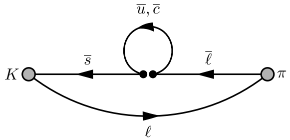

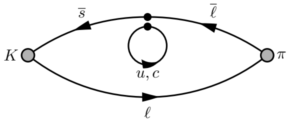

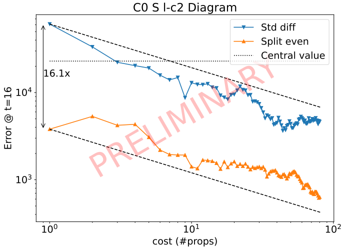

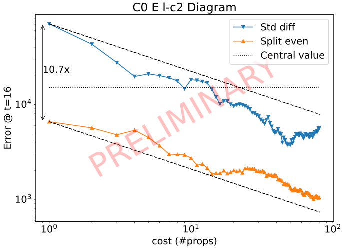

Plots: Raoul Hodgson (DESY)

- Exploratory tests suggest roughly an order-of-magnitude improvement in statistical uncertainty simply by swapping to a 'split-even' estimator for the GIM loop.
- **Highly preliminary:** plots based on 10 configurations.

Frequency-Splitting

- Another technique, builds on split-even: frequency-splitting[1].
- Rather than computing an $l - c$ loop, decompose into $\sum_i^{n-1}(q_i - q_{i+1})$, with $q_0 = l$ and $q_n = c$.
- Calculate each mass sub-range with the split-even estimator.
- Different statistical properties for each sub-range.
- Judiciously choosing a q_i set can allow computational effort to be concentrated on the noisiest contributions.

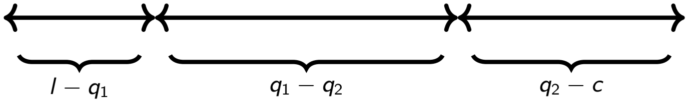

[1] Giusti *et al.* EPJC 79, 586 (2019) [arXiv:1903.10447]

$K^+ \to \pi^+\ell^+\ell^-$: Preliminary frequency-split variances

- Ex: using a strange mass to split the mass range.
- Reach the gauge noise for the heavier loops?
- Large ($\sim 30\times$!) gains for $l - s$ loop—not at gauge noise even at 80 hits.

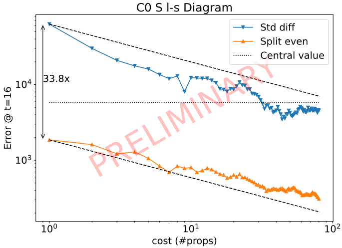

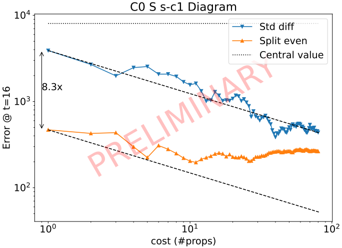

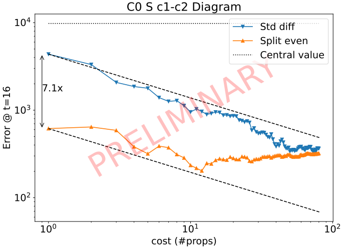

Plots: Raoul Hodgson (DESY)

Conclusions

- Disconnected QED diagrams are difficult to resolve.
- Diagrams at $\mathcal{O}(\alpha)$ have exploitable characteristics:
  $\rightarrow$ 'Burger' is short-distance dominated.
  $\rightarrow$ Others feature differences of single-propagator loops.
- The split-even estimator greatly improves efficiency of stochastic estimation, even at the physical point.
- Techniques also have applications beyond disconnected QED:
  $\rightarrow$ Potentially resolve physical-point $K^+ \rightarrow \pi^+\ell^+\ell^-$ amplitude

Backup

FLAG $f_{\pi^\pm}$, $f_{K^\pm}$ Citation List

Dowdall *et al.* PRD 88 (2013) 074504
Carrasco *et al.* PRD 91 (2015) 054507
Bazavov *et al.* PRD 98 (2018) 074512
Miller *et al.* PRD 102 (2020) 034507
Alexandrou *et al.* PRD 104 (2021) 074520
Follana *et al.* PRL 100 (2008) 062002
Bazavov *et al.* PoS LATTICE2010 (2010) 074
Durr *et al.* PRD 81 (2010) 054507
Blum *et al.* PRD 93 (2016) 074505
Durr *et al.* PRD 95 (2017) 054513
Bornyakov *et al.* PLB 767 (2017) 366–373
Blossier *et al.* JHEP 07 (2009) 043

FLAG f_D, f_{D_s} Citation List

Balasubramamian, Blossier EPJC 80 (2020) 5, 412
Carrasco *et al.* JHEP 03 (2014) 016
Davies *et al.* PRD 82 (2010) 114504
Bazavov *et al.* PRD 85 (2012) 114506
Boyle *et al.* JHEP 12 (2017) 008
Yang *et al.* PRD 92 (2015) 034517
Na *et al.* PRD 86 (2012) 054510
Bazavov *et al.* PRD 98 (2018) 074512
Carrasco *et al.* PRD (2015) 054507